PCCP

Accepted Manuscript

This is an *Accepted Manuscript*, which has been through the Royal Society of Chemistry peer review process and has been accepted for publication.

Accepted Manuscripts are published online shortly after acceptance, before technical editing, formatting and proof reading. Using this free service, authors can make their results available to the community, in citable form, before we publish the edited article. We will replace this *Accepted Manuscript* with the edited and formatted *Advance Article* as soon as it is available.

You can find more information about *Accepted Manuscripts* in the **Information for Authors**.

Please note that technical editing may introduce minor changes to the text and/or graphics, which may alter content. The journal's standard **Terms & Conditions** and the **Ethical guidelines** still apply. In no event shall the Royal Society of Chemistry be held responsible for any errors or omissions in this *Accepted Manuscript* or any consequences arising from the use of any information it contains.

Dynamic Article Links ▶

ARTICLE TYPE

Two-dimensional Structure Au Nanosheets Are Super Active for the Catalytic Reduction of 4-Nitrophenol **

Yan Zhang[a], Zhimin Cui[a], Lidong Li[a]*, Lin Guo[a]*, Shihe Yang[a,b]*

Two-dimensional structure Au nanosheets with a polygon morphology and controlled thicknesses of ~ 15 nm, ~ 35 nm, ~ 50 nm were successfully synthesized by a one-step solution reduction method. Scanning and transmission electron microscopy (SEM and TEM), selected area electron diffraction (SEAD) analyses, and X-ray diffraction (XRD) were used to thoroughly study the structure and the formation mechanism of the nanosheets. The catalytic activity of the Au nanosheets was investigated on the reduction of 4-nitrophenol (4-NP) by UV-visible absorption spectroscopy. Against all expectation, the Au nanosheets with such a big lateral (more than 1 μm) size exhibited superior catalytic activity on the selective reduction of 4-nitrophenol (4-NP) to 4-aminophenol (4-AP) in the presence of NaBH$_4$. On the other hand, the catalytic activity does closely depend on the thickness of the nanosheets, that is, it decreases with increasing thickness. The reaction can be completed in less than 1 min. when catalyzed by the Au nanosheets about 15 nm thick. The 100% conversion efficiency was further demonstrated after two catalytic cycles with the thinnest Au nanosheets.

1. Introduction

Gold, for quite a long time, had been considered as chemically inert and catalytically inactive because of its completely filled d-band.[1] However, when the size is reduced to the nanometer level, Au becomes highly active catalysts, even at low temperatures.[2-4] With the booming interest of exploring gold-based catalysts, smaller nanoparticles, due to their higher surface-to-volume ratios, are often prepared and used for catalytic reactions.[5-7] The downside of using smaller nanoparticles, however, is their tendency of aggregation driven by surface energy minimization, leading to undesirable reduction of their catalytic activities and reuse life-time. As

such, such small catalytic nanoparticles are often immobilized on appropriate supports[8,9] to prevent the aggregation. Recently, Ballauff et al. studied the catalytic reduction of 4-nitrophenol using metal nanoparticles immobilized in spherical polyelectrolyte brushes, which have an average size of approximately 2 nm.[4,10] Unfortunately, the use of supports often suffers from the failure to obtain highly dispersed and stable gold nanoparticle catalysts. Sometimes, the small nanoparticles leach out from the supports during the washing and recycling processes.

It is a common knowledge that the catalytic activity of nanoparticles rests with the active atoms on the surface, especially at certain highly under-coordinated and structurally distorted sites.[7,11-14] Recognizing that the catalytic activity of a metallic catalyst depends strongly on its surface properties. Yang's group controlled the morphology of catalytic nanostructures to regulate the exposed surfaces with distinct crystallographic planes while preserving the catalytically active sites.[13] Therefore, an emerging challenge is to design and produce Au nanoparticles with a big size, which is necessary for promoting the catalyst retention and the product separation, and at the same time, more active sites on the exposed surfaces.[1]

As we know that, two-dimensional nanomaterials are typically generated from bulk layered crystalline solids such as graphene, which consist of successive layers of covalently bonded atomic layer planes ranging from one to multiple atoms thick, separated successively by van der Waals gaps.[15-17] Owing to the super thin and flat structure of the two-dimensional nanomaterials, our Au nanosheet exhibits remarkable catalytic, optical and mechanical

properties.

In this work, we have succeeded in the synthesis of gold nanosheets with a micrometer diameter and a controllable nanometer scale thickness by a simple one-step solution method. Unexpectedly, these two-dimensional gold nanosheets showed very high catalytic activity to the reduction of 4-nitrophenol. The big size of two-dimensional structure, low catalyst loss, no aggregation, and easy recyclability make these gold nanosheets an ideal catalyst. Furthermore, the gold nanosheets with different thicknesses have shown different catalytic rates exhibiting a decreasing trend with increasing thickness of the nanosheets. The 100% conversion efficiency with the thinnest Au nanosheet after two catalytic cycles is also demonstrated.

2. Experimental Section

0.0015 g CTAB (cetyltrimethylammonium bromide) and 0.232 g PVP (polyvinylpyrrolidone,58000) were dissolved in 22 mL ethylene glycol. The solution was kept at the temperature of 90 □ for 15 minutes, and then 8 mL of $HAuCl_4$ solution with different concentration was added dropwisely, the solvent of which was dimethyl sulfoxide (DMSO). The reaction was completed in 120 min. Then the products were collected by centrifugation and washed with ethanol for three times. The thickness of the product Au nanosheets was controlled by the concentration of $HAuCl_4$ solution. When the concentration of $HAuCl_4$ solution is controlled from 5.0×10^{-3} to 1.5×10^{-3} M, the thickness of the Au nanosheets is varied from 15 nm to 50 nm, respectively.

The Au nanosheets with different thickness were used as catalyst to the reduction of 4-NP. The reaction was carried in a 3 mL spectrophotometer cell and the reaction process was measured in situ with the Uv-Vis spectrophotometer. Typically, 1.3 mL of 4-NP aqueous solution (2×10^{-4} M), 0.2 mL of the prepared Au nanosheets solution (1.7×10^{-2} M) was first added to the cell. Then 1.5 mL of $NaBH_4$ solution (8.0×10^{-2} M) was rapidly injected into the reaction solution. The yellow color of solution gradually vanished, indicating the reduction of 4-NP. The concentration of 4-NP was monitored by the UV-2550 spectrophotometer. For recycling experiment, Au nanocatalyst was collected by centrifugation of 10000 r/5 min after the reaction, washed two times with deionized water, and then reused.

Scanning electron microscopy (SEM) images were carried out at Quanta 250 FEG and JSM-7500F. High-resolution transmission electron microscopy (HRTEM) images were performed with a JEOL JEM-2100F microscope. UV-Vis spectra were acquired on a spectrophotometer (UV-2550,

Shimadzu).

3.Results and Discussion

Low and high-magnification of scanning electron microscopy (SEM) images of **Figure 1a, 1b** show that the obtained products are the regular-shaped sheets, such as triangular, hexagonal, and truncated triangular shaped. SEM image of higher magnificatioin (**Figure 1b**) shows that there are also a substantial number of nanosheets with few nanoparticles. Similar little nanoparticles have also be seen in the report of Huang et al.[18] and Long Jiang et al.[19], which might probably be related to the condition of high solution temperature, which favors the rapid formation of gold nanoparticles and facilitates particle fusion, the small particle sizes, and the capping action of the surfactant micelles. **Figure 1c, d** and **e** show TEM images of a single sheet with the shape of triangular, hexagonal, and truncated triangular, respectively. They show that each nanosheet is an integrated individual. The insets show the corresponding selected area electron diffraction (SAED) pattern of these nanosheets obtained with the electron beam perpendicular to the planar flat surface. The SAED pattern further reveals the single crystaline nature of gold nanosheets. The squared and triangled spots can be indexed to the {220} and 1/3{422} reflections, respectively. The reflection phenomenon of the forbidden 1/3{422} can be observed indicateing the presence of stacking faults in the {111} plane perpendicular to the electron beam. We may explain that this planar defect disrupts the fcc symmetry of gold and is responsible for the formation of an anisotropic, plate-like structure.
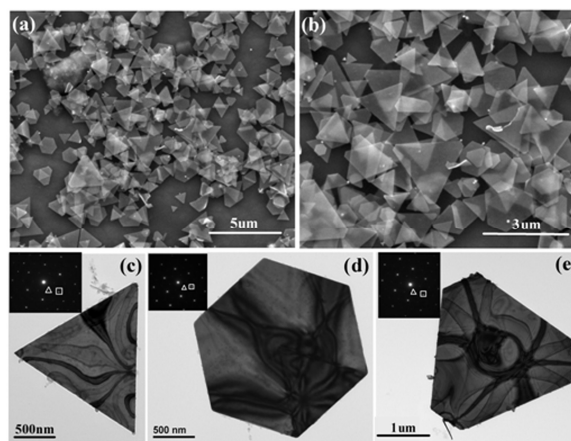
Figure 1 (a, b) Low and high magnification SEM images of the as-prepared Au nanosheets with the thickness ~ 15 nm. (c, d, e) TEM images of triangular, hexagonal, and truncated triangular plates acquired in figure 1a, 1b. The insets in (c), (d) and (e) show diffraction pattern

recorded by aligning the electron beam perpendicular to the flat faces of each plate. In the [111] zone axis, the diffracted spots are indexed to {220} (boxed spot) and 1/3{422} (triangled spot) Bragg reflections, corresponding to lattice spacing 1.44 and 2.50 Å, respectively.

The thicknesses of gold nanosheets can be controlled by the concentration of reactant. **Figure 2a~f** depicts the SEM images of Au nanosheets with different thicknesses. If the concentration of the reactant Au^{3+} is 1.5×10^{-3} M, the thickness of obtained gold nanosheets is about ~ 50 nm (**Figure 2a, d**). The SEM image (**Figure 2a**) of the dispersed nanosheets displays the nonuniformity of the products. Meanwhile, the corresponding cross section view of an individual nanosheet shows the thickness of product is about 50 nm (**Figure 2d**). When the Au^{3+} concentration was increased to 3.5×10^{-3} M, the morphology of the products is shown in **Figure 2b**, indicating the diameter of the nanosheets were in the range of 1 ~ 2 μm. And the thickness of Au nanosheets at this concentration is decreased to ~ 35 nm, which can be clearly measured from **Figure 2e**. When the concentration of Au^{3+} was further increased to 5.0×10^{-3} M, the diversity of the shapes can be clearly observed in **Figure 2c**, including triangular, hexagonal and truncated triangular-shaped. And the corresponding cross section view of the nanosheet reveals that the thickness of the as-synthesized Au nanosheets was even decreased to ~ 15 nm (**Figure 2f**). Based on above morphological studies, we conclude that that higher concentration of Au^{3+} solution leads to thinner Au nanosheets. More SEM images of Au nanosheets with different thickness are shown in figure S1. The synthesis of Au nanostructures and nanoplates was indeed reported by several groups. However, Au nanosheets with controlled thickness was still difficult to be obtained. In this manuscript, we developed an easy method to synthesize Au nanosheets with controlled thickness from 15 nm to 50 nm. More SEM images that show the difference of thickness of the Au nanoplates were added in the revised manuscript. Figure S2 exhibited the TEM images of 35nm and 15nm Au nanosheets. The clear lattice image indicates the high crystallinity of the Au nanosheets. A lattice spacing of 0.23 nm for the {111} planes can be readily resolved.

XRD analysis shown in **Figure 2g** supplies the further structure information of the Au nanosheets. The face-centered cubic (fcc) structure (JCPDS card no.65-2870) of gold crystal diffraction pattern was recognized from the exceedingly high peak at 38.2°, which can be indexed to the (111)-crystallographic planes of fcc gold nanocrystals. The overwhelmingly high intensity of (111) diffraction peak

indicates a certain predominance of the (111) facets on the formed nanosheets, and the the lower free energy of the (111) planes relative to the other planes may contribute to the higher catalytic and sensing activity.[20-22] It is worth noting that the XRD pattern of the Au nanosheets of 15 nm thickness is broaden visibly, which agrees well with that the Au nanosheets is thinner than 20 nm. The Au nanosheets were consisted of triangular, hexagonal and truncated triangular sheets over a range of size, reaching micrometer level. The UV-Vis spectrum of the nanosheets was shown in the figure S3. There is an absorption peak at 510 nm for the 15nm Au nanosheets and the adsorption gradually increased to the near-infrared area. The adsorption peak at 510 nm was shifted to short wavelength with the increase of the thickness of the nanosheets.

In the paper, the synthesis of Au nanosheets thickness controlling was mainly controlled by the concentration of $HAuCl_4$ solution. Using this method, the less amount of Au nanosheet seeds were formed by the lower concentration of $HAuCl_4$ solution. As the reaction progressed, those nanosheet seeds were able to grow into thicker nanosheets. While the higher concentration of $HAuCl_4$ solution easily leaded to the more amount of Au nanosheet seeds, which grown into thinner nanosheets.[23-26]

So far, scientists have done a lot of work to deal with the interesting issue on the gold nanosheets, especially the simple aqueous solution synthesis.[27-30] Synthesizing Au nanosheets and the control of their edge length or shape have been realized well by some reported work, however, only a few systems produce gold plates with thickness controlling.[31] Therefore, searching for a synthesis method with controllable thicknesses for gold nanosheets is worthwhile. Herein, we propose a novel synthesis method with following advantages over other people : (1) the thickness can be controlled by simply adjusting the concentration of $HAuCl_4$; (2) the preparation method is convenient, efficient and operated under a mild condition of 90□ and the solvent has reducibility by itself with no need to add any other reducing agents, which reduces the influence of the reductants and simplifies the fabrication process. (3) It is also fast and stable, reusable and economical with no need for expensive additives.

The catalytic activity of ~50 nm Au nanosheets, 35 nm Au nanosheets and ~15 nm Au nanosheets toward 4-NP reduction is convincingly demonstrated by the time-dependent UV−vis absorption spectra of the reduction process, as shown in **Figure**

3a, b and **c**, respectively. **Figure 3** displays the typical evolution of the UV-vis spectra with time in the presence of Au nanosheets. Upon the addition of $NaBH_4$ was added to the solution containing the Au nanosheet catalysts and 4-nitrophenolate ions formed, the height of the absorption peak 4-NP at 400 nm successively decreased as the reaction proceeded. Meanwhile, a new absorbance peak centered at ~ 300 nm appeared, corresponding to the product (4-AP). Curve in **Figure 3c** indicates the catalytic reduction with the ~15 nm Au nanosheets was fully completed within 90 seconds, which is much faster than the ~50 nm Au nanosheets (more than 900 seconds) and ~35 nm (less than 900 seconds), as shown in **Figure 3a, b**. The catalytic reduction was much faster in the case of ~35 nm Au nanosheets compared to that of ~50 nm Au nanosheets at the same time. It is worth noting that gas bubbles of H_2 formed by the decomposition of $NaBH_4$, may impede the absorbance measurements during the reaction, leading to a shift of UV-vis spectra and missing isosbestic points.[10]
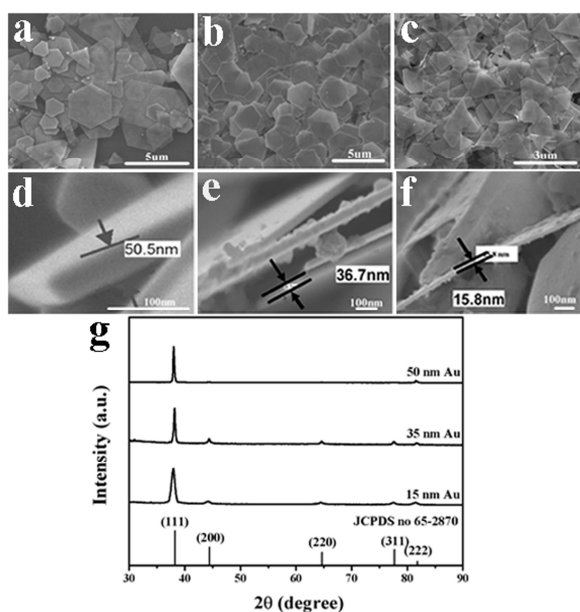
Figure 2 The SEM images of Au nanosheets at three thicknesses: (a, d) ~ 50 nm; (b,e) ~ 35 nm; (c,f) ~ 15 nm; (g) XRD patterns of Au nanosheets with different thicknesses.

Figure 3d shows the typical conversion curves versus time in the presence of Au nanosheets with different thickness. For every catalyst with a certain thickness, an induction time is observed from the conversion curve, during which no reduction occured. According to the literature, the induction time is related to the a slow surface reconstruction of the nanoparticles to become active catalysts, and the rate of the induction time is directly related to the surface reaction,[4,10] then the reaction

becomes stationary. As shown in **Figure 3d**, the induction time of the Au nanosheets with the thickness of 50 nm is about 200 seconds, and it became shorter as the thickness of the Au nanosheets decreases, indicating that there are more active sites on the thinner nanosheets. The reaction of 4-nitrophenolate catalyzed by thinnest Au nanosheets ~15 nm can reach 100% conversion in less than 100 seconds, and the Au naosheets with medium thickness of ~35 nm reach more than 95% conversion in less than 900 seconds. Furthermore, only 60% conversion could be reached by using thickest Au nanosheets of ~50 nm. In this reaction, the same amount of Au nanosheets for different thicknesses were used, the turnover frequency (TOF) of the reaction can be calculated as 0.050 s^{-1}, 0.0050 s^{-1} and 0.0030 s^{-1} for ~15 nm, ~35 nm and ~50 nm Au nanosheets, respectively. It is worth noting that all three nanosheets are much more active than the controlled Au nanoparticles with diameter of 125 nm, which leads to only 23% conversion within 900 seconds.
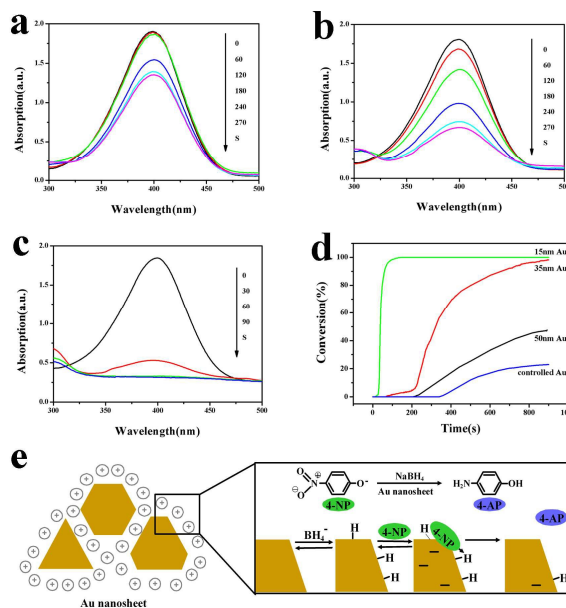
Figure 3.(a~d) UV-vis absorption spectrum of 4-NP by using Au nanosheets with different thickness at increasing times: (a)Au nanosheets with thickness of ~50 nm; (b) Au nanosheets with thickness of ~35 nm; (c) Au nanosheets with thickness of ~15 nm; (d) Time dependence of 4-nitrophenolate conversion in reduction reaction by using different Au nanosheets: controlled Au refers to the nanoparticles with a diameter about125 nm; (e) The scheme of reaction mechanism (Langmuir-Hinshelwood mechanism) for the reduction of 4-NP to 4-AP by borohydride in the presence of Au nanosheet.

Based on the above results from **Figure 3a~d**, the reaction mechanism of the catalytic reduction can be explained by the form of Langmuir−Hinshelwood (LH) model [4,32] illustrated in **Figure 3e**. The transversion of catalysis reaction can be

4

described as follows: Firstly, the borohydride ions adsorb on the surface of the Au nanosheet and react with the gold. Secondly, surface-hydrogen species are transfered to the surface of Au nanosheet. Of note, the whole process of above is reversible.[10,32] Along with the 4-nitrophenol molecules are adsorbed on the surface of the Au nanosheet, this reversible step is accompanied with the next procedure, in which the reactants rapidly diffuse to the surface of Au nanosheet, leading to a balance of the adsorption/desorption. When the reaction between the adsorbed 4-NP and the surface-hydrogen species takes palace, the rate-determining step of reduction of 4-nitrophenol has been completed. The product, 4-aminophenol, diffuse to the solution, leaving a free Au nanosheet surface, making up a complete cycle of catalysis. The chemical equation is as follows:
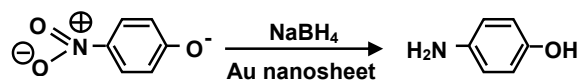
Apparently, the thinner nanosheets have lager specific surface area than thicker ones, which is favorable for the catalytic activity. Besides that, the SEM images (**Figure 2d~f**) shows that there are plenty of small bumps on the surface of the 15 nm Au nanosheets, indicating the surface roughness increases as the thickness of the nanosheets decreases. Generally, the rougher surfaces should possess more surface defects and provide more active catalytic sites, which lead to the best catalytic activity for the thinnest Au nanosheets.

One of the major advantages of these Au nanosheet catalysts is that they are easily reusable due to their big size. **Figure 4a, b, c** show the reusability of the different Au nanosheet catalyst for the reduction 4-NP with NaBH4. It can be observed that, after 2 cycles, the catalytic efficiency remained almost unchanged for all the three Au nanosheets. During the catalytic or separation processes, Au nanosheets are not deactivated or poisoned and could be recovered almost completely. The results prove that the as-prepared Au nanosheets could be ideal catalyst that have both high activity and stability, especially compared with some metal nanoparticles that suffer the drawback of surface oxide to lose activity[33,34] or AuNPs that suffer the aggregation to decrease reduction of catalytic activities.

The thickness of Au nanosheets keep almost unchanged during the catalytic process as showed in the figure S4. Different damage to the morphology of the Au nanosheets with different thickness happened due to the repeatedly sample

washing. The edges and margins of the used thickest Au nanosheet keep nearly the same morphology as before. As the decreasing of the thickness, the edges and margin of the thinner samples show the more chipped morphology, the reason for which is probably due to the reducing of the strength and hardness in the thinner Au nanosheets.
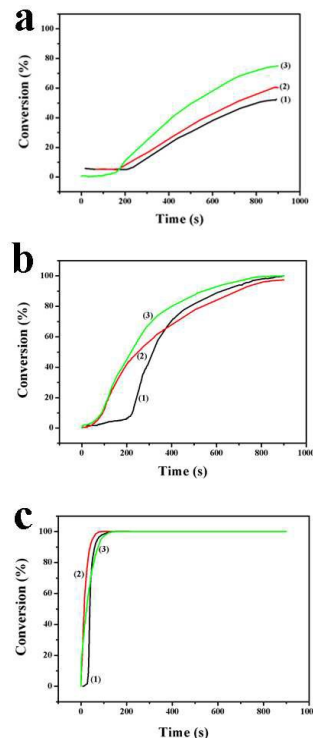
Figure 4. Reusability test of the Au nanosheets for the reduction of 4-NP with NaBH4: (a) Au nanosheets with the thickness of ~50 nm; (b) Au nanosheets with the thickness of ~35 nm; (c) Au nanosheets with the thickness of ~15 nm; (1) recoverable reusability for the first time; (2) recoverable reusability for the second time; (3) recoverable reusability for the third time.

The thinnest thickness of ~15 nm Au nanosheets and ordinary Au nanoparticles of around 125 nm were also investigated the SERS behaviors in figure S5. Particularly, the SERS intensities of the ν CS mode at 1076 cm^{-1} and ν CC band at 1587 cm^{-1}, the thinnest thickness of ~15 nm Au anosheets substrate gain larger enhancement than the ordinary Au nanoparticles substrate. This result suggests that the thinnest thickness of ~15 nm Au nanosheets obtain larger enhancement and could be used as an ideal active SERS substrate. The SEM of the compared Au nanoparticles is shown in figure S6.

FT-IR spectra in Figure S7 were recorded to identify the possible groups. In the spectra (a), vibrational frequencies of 1280 cm^{-1} and 1590 cm^{-1} is obtained for symmetric and

antisymmetric NO stretching modes, respectively. In the case of figure (b), the Vasym(NO) and Vsym(NO) are disappeared instead of the vibrational frequencies of 3280 and 3180 cm^{-1} are generated for the symmetric and antisymmetric NH stretching modes, respectively. Besides, we know that 4-NP can convert to the single product 4-AP.According to conversion rate, when it reaches to 100%, we think the product is 4-AP.

Conclusion

In conclusion, by simply controlling Au^{3+} concentration, two-dimensional Au nanosheets with different thickness were successfully synthesized through a simple one-step method in a quite high yield. SEM and TEM images demonstrated that these Au nanosheets were composed of several regular polygons, such as triangular, hexagonal, and truncated triangular. These nanosheets were further proved to have single crystal nature. The Au nanosheets with the thickest thickness of 15 nm showed highest catalytic activity to the reduction of 4-nitrophenol to 4-aminophenol (4-AP) at room temperature. The reaction can be completed in less than 90 seconds. And the catalytic activity is closely related to the thickness of the Au nanosheets, i.e. the activity increases as the thickness decreases. Moreover, the Au nanosheets can be recovered easily and can be reused without any deactivation or poisoning, demonstrating the high stability and superior catalytic properties of the Au nanosheet catalysts. Furthermore, the as-prepared gold nanosheets with different thickness are promising for the potential application in sensing, imaging and etc.

^{a} *School of Chemistry and Environment, Beihang University, Beijing 100191, PR China. lilidong@buaa.edu.cn; guolin@buaa.edu.cn*
^{b}*Department of Chemistry, The Hongkong University of Science and Technology, Clear Water Bay, Kowloon, HongKong, China*

Reference

1   H. Wu, X. Huang, M.-M. Gao, X.-P. Liao and B. Shi, *Green Chem*, 2001, **13**, 651.

2   A. Stephen K. Hashmi and Graham J. Hutchings, *Angew. Chem. Int. Ed*, 2006, **45**, 7896.

3   G. J. Hutchings, M. Brust and H. Schmidbaur, *Chem. Soc. Rev.*, 2008, **37**, 1759.

4   S. Wunder, Y. Lu, M. Albrecht and M. Ballauff, *ACS Catal.*, 2011, **1**, 908.

5   S. C. Davis and K. J. Klabunde, *Chem. Rev.*, 1982, **82**, 153.

6   S. Vajda1, M. J. Pellin, J. P. Greeley, C. L. Marshall, L. A. Curtiss, G. A. Ballentine, J. W. Elam, S. Catillon-Mucherie, P. C. Redfern, F. Mehmood and P. Zapol, *Nature Mater.*, 2009, **8**, 213.

7   N. Hu, J.-Y. Yin, Q. Tang and Y. Chen, *Journal of Polymer Science Part A: Polymer Chemistry*, 2001, **49**, 3826.

8   A. G. Boudjahem, S. Monteverdi, M. Mercy and M. M. Bettahar, *Journal of Catalysis*, 2004, **221**, 325.

9   J. W. Yoo, D. J. Hathcock and M. A. El-Sayed, *Journal of Catalysis*, 2003, **214**, 1.

10   S. Wunder, F. Polzer, Y. Lu, Y. Mei and M. Ballauff, *J. Phys. Chem. C,* 2010, **114**, 8814.

11   J. Zeng, Q. Zhang, J. Y. Chen and Y. N. Xia, *Nano Lett.*, 2010, **10**, 30.

12   M. A. Mahmoud, F. Saira and M. A. El-Sayed, *Nano Lett.*, 2010, **10**, 3764.

13   H. Lee, S. E. Habas, S. Kweskin, D. Butcher, G. A. Somorjai and P. D. Yang, *Angew. Chem.*, 2006, **118**, 7988.

14   R. Narayanan and M. A. El-Sayed, *J. Am. Chem. Soc.*, 2004, **126**, 7194.

15   Kristie J. Koski and Yi Cui, *ACS NANO*, 2013, **7**, 3739.

16   Xiao Huang, Zongyou Yin, Shixin Wu, Xiaoying Qi, Qiyuan He, Qichun Zhang, Qingyu Yan, Freddy Boey, and Hua Zhang, *small*, 2011, **7**, 1876.

17   Xiao Huang, Xiaoying Qi, Freddy Boey, and Hua Zhang, Chem. Soc. Rev., 2012, **41**, 666.

18   W.-L. Huang, C.-H. Chen and M. H. Huang, *J. Phys. Chem. C*, 2007, **111**, 2533.

19   A. A. Umar, M. Oyama, M. M. Salleh and B. Y. Majlis, *Crystal Growth & Design*, 2009, **9**, 2835.

20   M. Wang, L. Wang, G. Wang, X. Ji, Y. Bai, T. Li, S. Gong, and J. H. Li, *Biosensors and Bioelectronics*, 2004, **19**, 575.

21   Da Chen, Geng Wang, and Jinghong Li, *J. Phys.*

Chem. C, 2007, **111**, 2351.

22 M. Wang, C. Sun, L. Wang, X. Ji, Y. Bai, T. Li, and J. H. Li, *J. Pharmaceutical and Biomedical Analysis*, 2003, **33**, 1117.

23 Xiao Huang, Shaozhou Li, Yizhong Huang, Shixin Wu, Xiaozhu Zhou, Shuzhou Li, Chee Lip Gan, Freddy Boey, Chad A. Mirkin and Hua Zhang, *Nat. Commun.*, 2011, **2**, 292.

24 Xiao Huang, Hai Li, Shaozhou Li, Shixin Wu, Freddy Boey, Jan Ma, and Hua Zhang, *Angew. Chem. Int. Ed.*, 2011, **50**, 12245.

25 Zhanxi Fan, Xiao Huang, Chaoliang Tan and Hua Zhang, *Chem. Sci.*, 2015, **6**, 95.

26 Xun Hong, Chaoliang Tan, Junze Chen, Zhichuan Xu and Hua Zhang, *Nano Res.*, 2015, **8**, 40.

27 A. A. Umar, M. Oyama, M. M. Salleh and B. Y. Majlis, *Crystal Growth & Design*, 2010, **10**, 3694.

28 G. H. Lin, W. S. Lu, W. J. Cui and L. Jiang, *Crystal Growth & Design*, 2010, **10**, 1118.

29 C. S. Ah, Y. J. Yun, H. J. Park, W.-J. Kim, D. H. Ha and W. S. Yun, *Chem. Mater.,* 2005, **17**, 5558.

30 L. Au, B. Lim, C. Peter, Y.-S. Jun and Y. N. Xia, *Chem. Asian J.*, 2010, **5**, 123.

31 H. L. Qin, D. Wang, Z. L. Huang, D. M. Wu, Z. C. Zeng, B. Ren, K. Xu and J. Jin, *J. Am. Chem. Soc.*, 2013, **135**, 12544.

32 B. Baruah, G. J. Gabriel, M. J. Akbashev and M. E. Booher, *Langmuir*, 2013, **29**, 4225.

33 M. Gratzel and A. J. Frank, *J. Phys. Chem.*, 1982, **86**, 2964.

34 Y.-C. Chang and D.-H. Chen, *Journal of Hazardous Materials*, 2009, **165**, 664.

8